Available online at www.sciencedirect.com
SCIENCE DIRECT®
Journal of Nuclear Materials 349 (2006) 107–118
journal of nuclear materials
www.elsevier.com/locate/jnucmat

Modelling of bituminized radioactive waste leaching. Part II: Experimental validation

B. Gwinner [b], J. Sercombe [a,*], C. Tiffreau [c], B. Simondi-Teisseire [d], I. Felines [a], F. Adenot [a]

[a] *Commissariat à l'Energie Atomique (C.E.A.), Direction de l'Energie Nucléaire, Département de Traitement et de Conditionnement des Déchets, Service des Procédés de Décontamination et d'Enrobage, 13108 Saint-Paul-Lez-Durance, France*
[b] *Institut National Polytechnique de Lorraine (I.N.P.L.), 1, rue Granville, 54000 Nancy, France*
[c] *Commissariat à l'Energie Atomique, Direction de l'Energie Nucléaire, Département de Technologie Nucléaire, Service de Modélisation des Transferts et Mesures Nucléaires, 13108 Saint-Paul-Lez-Durance, France*
[d] *Institut de Radioprotection et de Sûreté Nucléaire, 13108 Saint-Paul-Lez-Durance, France*

Received 11 November 2004; accepted 14 October 2005

Abstract

This paper presents experimental work aiming at studying the behaviour of leached bituminized waste materials and the development of a saline solution-filled pore structure (called permeable layer) in the materials. Standard leach tests are performed on two synthetic BW materials containing different soluble salt contents and leached by solutions of varying chemical activities. The water uptake and the sodium nitrate leach rates are measured continuously during the tests. Porosity profiles are obtained from ESEM image analyses performed on the same BW samples leached during periods of varying durations. These experimental results provide a precise description of the internal structure of BW materials during leaching. The impact of the leaching duration, of the soluble salt content, and of the chemical activity of water in the leachant on the overall behaviour of leached BW materials is by this way assessed and compared to the theoretical trends presented in Part I of this paper.

PACS: 81.90.+c

1. Introduction

In Part I of this paper, a constitutive model called COLONBO describing the main phenomena taking place in leached BW materials has been presented. Analytical expressions have been derived which point out the main material and environmental parameters (soluble salt content of the BW material, chemical activity of water in the leachant) and their impact on the overall behaviour of leached BW materials (water uptake, salt release, thickness of the permeable layer, etc.). One of the main

* Corresponding author. Tel.: +33 4 42 25 30 72; fax: +33 4 42 25 46 15.
E-mail address: sercombe@cea.fr (J. Sercombe).

0022-3115/$ - see front matter © 2005 Elsevier B.V. All rights reserved.
doi:10.1016/j.jnucmat.2005.10.019

assumption at the origin of the constitutive model is that BW's leachability, that is to say, salt and radionuclides release, depends on the development of a solution-filled pore structure and on its progression in the material [4,12].

Most of past studies concerning BW leaching include data on salts and/or radionuclides release [1–13], obviously because of their importance with regards to the surrounding environment (engineering or geologic barriers). Only part of them include informations concerning the water uptake and the associated swelling of leached BW materials [2,4,6,7,9,12,13] in spite of their relevance with respect to the release of elements and correlation with the development of a pore structure in the leached material. To the authors knowledge, no study has been dedicated to the experimental quantification of the porous structure which forms and develops in leached BW materials and is at the origin of BW's leachability.

In this paper (Part II), experimental results aiming at describing the evolution of the porous zone (thickness, pore distribution, maximum porosity) which develops in leached BW materials are presented. They are obtained from standard leach tests and ESEM observations performed at different times on two different BW materials leached by solutions of various chemical activities. The experimental results are then compared to the theoretical trends given by the constitutive model described in Part I of this paper.

2. Experimental program

2.1. Preparation of synthetic BW samples

To study the evolution of the pore structure of BW during leaching, non-radioactive specimens have been synthesized using a distilled Viatotal 70/100 bitumen. The main characteristics of this 'soft' bitumen are summarized in Table 1.

The main steps of the industrial process used at the COGEMA La Hague plant (called STE3) in France to solidify radioactive liquid concentrates (effluents) originating from fuel reprocessing units have been reproduced at laboratory scale in order to elaborate non-radioactive representative sludges. The preparation consist in adding successively to an initial nitric concentrate (HNO_3) the following reagents: H_2SO_4, NaOH, $Ba(NO_3)_2$, used in the industrial process to capture radioactive strontium elements, PPFeNi (a nickel and potassium preformed precipitate), incorporated in the industrial process to fix cesium, Na_2S and $CoSO_4$, used in the industrial process to immobilize ruthenium radionuclides. After two decantations and removal of the floating on the surface, the remaining sludge is ready for incorporation in the bitumen matrix. From the HNO_3 concentration in the initial solution depends the final $NaNO_3$ content of the sludge and of the BW materials. Initial nitric solutions with HNO_3 concentrations of 0.5 N (mol/l) and 1 N have been used in this study to produce BW materials with two different $NaNO_3$ contents. The composition of a typical STE3 sludge (HNO_3 0.5 N) is given in Table 2.

The BW have been prepared as follows. Bitumen is first heated at 140 °C in a temperature controlled GUEDU steel mixer with a capacity of 2 l. Liquid sludges are then progressively injected at a constant rate by a peristaltic pump. Temperature (140 °C) and stirring are maintained until evaporation of water is completed. The end of the procedure is checked by collecting continuously vapor water in a condenser. Samples of BW weighting around 1 kg are produced by this process in about 5 h. In this experimental study, two BW were synthetized, differing mainly by the quantity of incorporated soluble salts ($NaNO_3$ and Na_2SO_4), as shown in Table 3.

2.2. Characterization of the synthetic BW samples

In order to check the homogeneity of the cast BW samples, which proved to be of great importance in the past for the reliability of experimental

Table 1
Characteristics of the Viatotal 70/100 bitumen

Density at 25 °C	1–1.1
Softening point (°C)	45–51
Penetration depth (0.1 mm)	70/100
Ductility (cm)	>100

Table 2
Composition of a typical STE3 sludge (HNO_3 0.5 N) from the La Hague plant in France (wt%)

$BaSO_4$	46%
PPFeNi	9%
CoS	10%
$NaNO_3$	28%
Na_2SO_4	5%

Table 3
Densities, total salt and soluble salt contents obtained for the two bituminized wastes (STE3 0.5 N and STE3 1 N)

Bituminized waste	Density (g/cm^3)	Total salt content (wt%)	Soluble salt content (wt%)
STE3 0.5 N	1.4 (estimated)	$(37.9 \pm 0.8)\%$	$(8.6 \pm 0.3)\%$
STE3 1 N	1.41 ± 0.03	$(42.1 \pm 2.8)\%$	$(17.3 \pm 0.8)\%$

data, four different tests have been carried out on small fractions of the samples:

- The density of the BW specimen has been measured using a picnometer and ethanol.
- The total salt content of the BW samples has been estimated as follows. First, the specimens are mixed with toluene till complete dissolution of the bitumen. The salts are then separated from the toluene–bitumen filled solution by centrifugation. Finally, the salts are dried at 70 °C and weighted.
- A chemical analysis of the salts has been made for each BW specimen. The soluble and insoluble salts obtained after dissolution of the bitumen matrix in toluene are separated with a SOXHLET. Soluble salts are then analyzed by ionic chromatography and insoluble salts by atomic absorption spectrometry or inductive coupled plasma atomic emission spectrometry.
- Microscopic observations with an Environmental Scanning Electron Microscope (ESEM) have been made to check visually the salt distribution in the BW samples.

The obtained experimental results are summarized in Table 3.

The small dispersion obtained concerning the different properties of the BW samples demonstrate the homogeneity of the cast specimen. STE3 0.5 N contains around 8% soluble salts, STE3 1 N, 17% (0.5 N and 1 N refer to the HNO_3 concentration in the initial solution used to produce the sludge). This is the main difference between the two types of tested BW, the total salt contents being fairly identical (38% and 42%). ESEM observations of unleached specimen are given in Fig. 1.

In Fig. 1, the different salts can be distinguished: grey cristals correspond to $NaNO_3$, white particles to $BaSO_4$, the dominant element. The dark grey background is bitumen. Based on these observations, the mean size of $NaNO_3$ crystals and $BaSO_4$ particles have been estimated at 10 and 1 μm, respectively. The size of the salt particles appeared in past studies to be a parameter of great importance with regards to the behaviour of leached BW materials.

2.3. Pore structure analyses

The experimental program was set up in order to provide an in-depth study of the pore structure evolution of BW materials during leaching. The mathematical description of the phenomena given in Part I of this paper has shown that the chemical activity of water in the leachant and the soluble salt content were key-parameters with respect to leaching. The experimental program focused therefore on the pore structure of the permeable layer with the goal of studying its evolution with regards to three main parameters:

- The duration of the leaching process, to verify that leaching kinetics follow square root of time laws. Note that this result, in spite of its evidence for diffusion controlled processes, has not been obtained in all the studies concerned with BW leaching [2,4]. However, in most of them, water

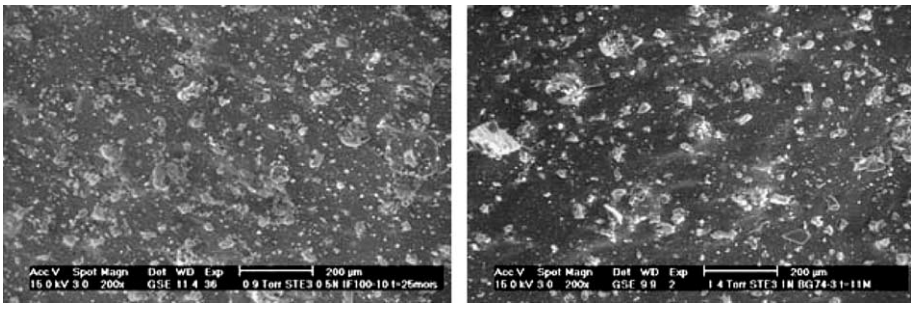

Fig. 1. ESEM observations of the two studied BW (STE3 0.5 N left and STE3 1 N right).

uptake, salt or radionuclides releases were found to follow uni- or bilinear square root of time laws [1,3,5,6,12,13].

- The chemical activity of water in the leachant. This parameter is of great importance since the chemical activity gradient is the driving force for water diffusion in the permeable layer of leached BW materials [4,7,13]. In this paper, test results concerning BW samples immersed in aqueous solutions with chemical activities varying between 0.74 (0.74 being the chemical activity of water in a $NaNO_3$ saturated solution) and 1 are presented.
- The soluble salt content. It theoretically plays a major role with respect to the progression of the permeable layer, see Eq. (25) in Part I. Its impact on swelling and salt/radionuclides release is furthermore confirmed by many past studies [1,8,11–13].

Leached BW samples consist of cylinders with a thickness of 1 cm and a diameter of 3.4 cm. To prepare the samples, small quantities (about 10 g) of BW materials cast with the GUEDU mixer are placed in cylindrical plastic tubes and then heated for half an hour at 60–65 °C to flatten their upper surface. Next, the BW samples are recovered by 20 ml of an aqueous solution with a fixed chemical activity. The chemical activity is controlled by the addition of a specific quantity of potassium iodine (KI). Samples can be classified in two types: Renewed (R) samples where the leachant is regularly changed and analyzed, Non-Renewed (NR) samples where the leachant is not changed. Renewed samples are used to follow the water uptake and the release of sodium nitrate. Water uptake is measured by weighting the plastic tubes and the BW samples after carefull drying of the leached surfaces with cotton-wool. Regular analyses of the leachant by ionic chromatography are used to measure the quantity of leached nitrate ions (NO_3^-) and hence of $NaNO_3$. Non-Renewed samples are dedicated to ESEM observations. The surface to volume ratio ($0.45\ cm^{-1}$) ensures however little variation of the leachant during the tests performed on NR samples.

To quantify the porosity and the pore distribution in the permeable layer of the synthetic BW samples, a semi-automatic experimental method based on the analysis of ESEM images has been developed at the laboratory [14,15]. At regular time intervals, and for the different leaching conditions, BW samples and their containment (plastic tubes) are frozen at −12 °C. At that temperature, BW samples tend to be solid and brittle. They are then fractured mechanically in two half cylinders in a direction perpendicular to the leached surface. The quality of the fracture plane allows one to perform direct ESEM observations of the surface, starting from the leached extremity of the samples. A mechanical-based preparation was prefered to sawing which can lead to some local elevation of the temperature with the risk of modifying the pore structure in the permeable layer. ESEM operating conditions have been optimized for the observation of BW samples as follows:

- beam voltage which controls the quality of the images is set at 12–15 kV (high resolution),
- pressure and temperature in the observation room are continuously kept at 200–270 Pa and −5 °C, respectively, in order to avoid the melting or a too important dessication of the frozen BW samples,
- a 200× magnification (leading rectangular images of $1231 \times 836\ \mu m$) is chosen as a compromise between a good representativity with respect to the maximum size of the pores (≈100–200 μm) and a limited number of images per leached BW sample. Note that the minimum pore diameter that can be observed with this magnification is 9–10 μm.

A typical image of the permeable layer of a leached BW sample obtained by ESEM is shown in Fig. 2.

Next step consist in reprocessing the grey images obtained by ESEM to generate binary images where

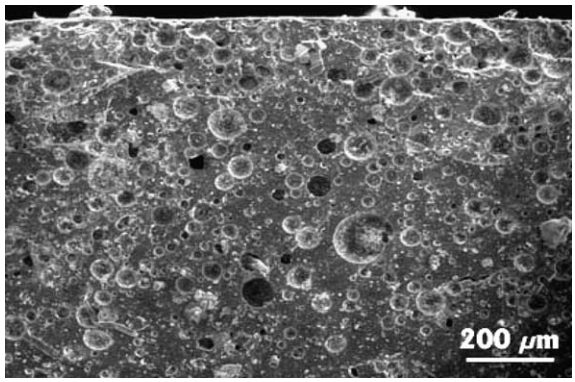

Fig. 2. ESEM observation of a STE3 1 N sample leached during 11 months by a solution of chemical activity 0.89, magnification ×200.

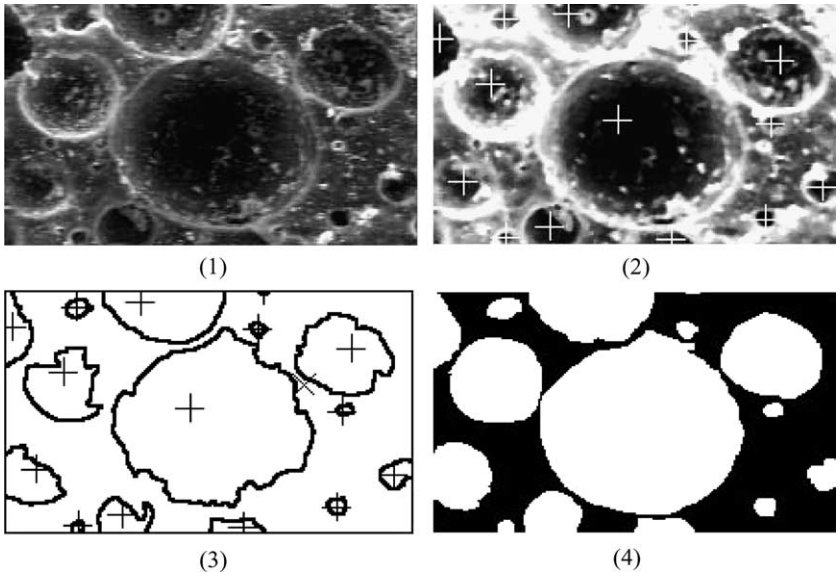

Fig. 3. Generation of binary images: (1) ESEM image, (2) pore marking, (3) automatic detection of pore borders, (4) manual correction of pore borders.

pores appear white and the bitumen matrix black. Due to the small contrast that exist between the bitumen phase (dark grey) and the solution-filled cavities (also dark grey), an automatic segmentation of grey levels is not possible. In consequence a manual marking of pores had to be employed prior to the use of an automatic program (OPTIMAS software) based on watershed algorithms [14,16]. Finally, the resulting binary images are corrected by a manual redefinition of the pore borders. Fig. 3 illustrates the different phases of the segmentation process. Fig. 4 shows the binary image resulting from the reprocessing of the ESEM picture presented in Fig. 2.

By estimating the number of white pixels and the total number of pixels, the pore volume of the permeable layer of leached BW can be assessed. By repeating this operation in layers of BW of equal thickness (100–200 μm), starting from the leached surface of the samples, porosity profiles can be plotted, as shown in Fig. 5.

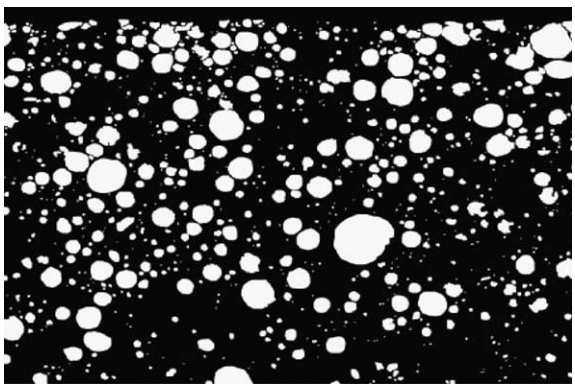

Fig. 4. Binary image of a STE3 1 N sample leached during 11 months by a solution of chemical activity 0.89, magnification 200×.

3. Leach tests results

3.1. Water uptake

Experimental results concerning the water uptake of STE3 0.5 N and STE3 1 N samples leached by solutions in which the chemical activity of water varies between 0.88 and 1 are presented in Figs. 6 and 7, respectively. The curves consist of average values obtained from three identical BW samples leached in the same conditions.

Obviously, the plots of Figs. 6 and 7 are linear functions of the square root of time ($days^{0.5}$). This confirms that water ingress in BW specimen is mainly controlled by diffusion processes. Consistent with the constitutive model presented in Part I of this paper (see Eq. (26) in Part I), the water uptake increases with the chemical activity of water in the leachant a_o, particularly when the chemical activity of water in the leachant exceeds 0.95–0.97. This

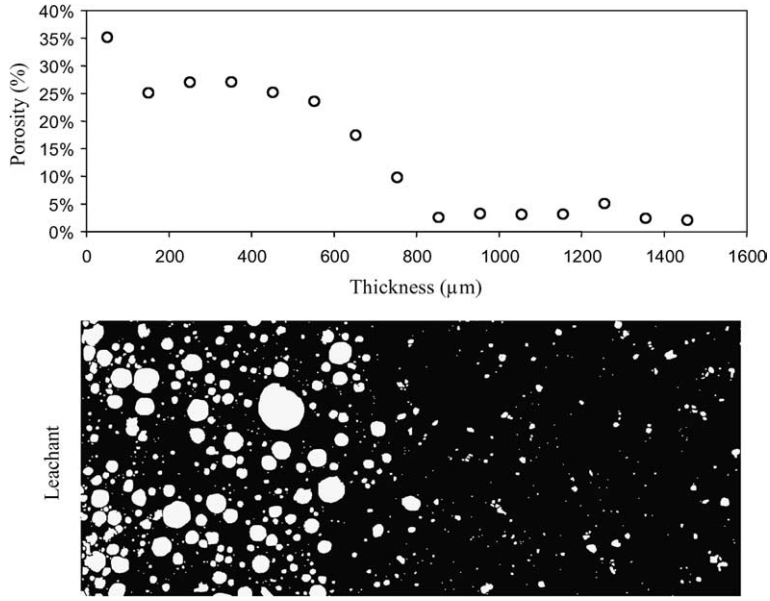

Fig. 5. Binary image and porosity profile in the permeable layer of a STE3 1 N sample leached during 11 months by a solution of chemical activity 0.89.

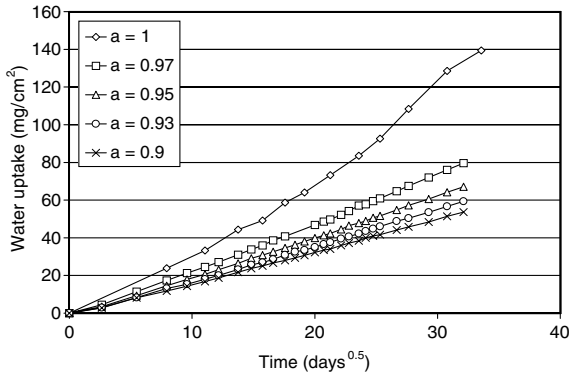

Fig. 6. Water uptake of STE3 0.5 N samples leached by solutions in which the chemical activity of water a_o varies between 0.9 and 1.

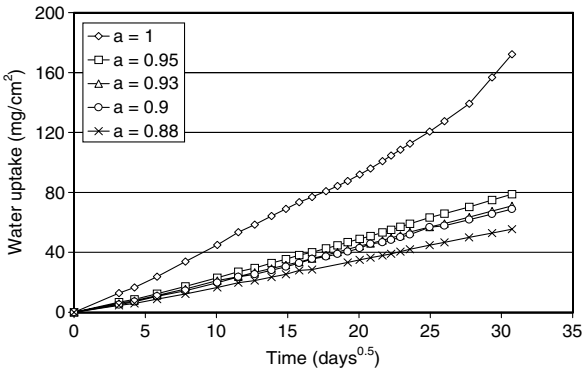

Fig. 7. Water uptake of STE3 1 N samples leached by solutions in which the chemical activity of water a_o varies between 0.88 and 1.

behaviour is in accordance with the water/$NaNO_3$ equilibrium curve of Fig. 4, Part I, which presents a substancial rise when the chemical activity of water reaches 0.9–0.95. It can be attributed to the important quantity of water that is needed to achieve a given chemical equilibrium in the pores of the permeable layer when the chemical activity of water is close to 1 (pure water). These results demonstrate that, the higher the chemical activity of water in the leachant, the greater the quantity of water needed to the progression of the permeable layer in leached BW materials and hence the higher the water uptake of the specimen.

The comparison between Figs. 6 and 7 also shows that the water uptake rates of the STE3 1 N samples are generally greater than those of the STE3 0.5 N samples. Water uptake rates of STE3 0.5 N samples are, respectively, equal to 3.8, 2.0 and 1.6 $mg/cm^2/days^{0.5}$ when leached in solutions of chemical activities equal to 1, 0.95 and 0.9. In comparison, the water uptake rates of STE3 1 N samples leached by similar solutions are, respectively, equal to 4.9, 2.5 and 2.2 $mg/cm^2/days^{0.5}$. This result illustrates the theoretical increase of the water uptake rate with the soluble salt content of the BW materials (8% for STE3 0.5 N and 17% for STE3

1 N), as predicted by the constitutive model presented in Part I (see Eq. (26) in Part I).

3.2. Sodium nitrate release

Experimental results concerning the sodium nitrate release of STE3 0.5 N and STE3 1 N samples leached by solutions in which the chemical activity of water varies between 0.88 and 1 are presented in Figs. 8 and 9, respectively. The curves consist again of average values obtained from three identical BW samples leached in the same conditions.

The $NaNO_3$ released quantities show a reasonably good linearity when plotted in function of the square root of time $\sqrt{t}$, demonstrating the diffusion-controlled nature of soluble salt leaching in BW materials. The general tendency is of a greater release rate when the chemical activity of water in the leachant increases. When comparing STE3 0.5 N and STE3 1 N samples, it also appears that the quantity of leached $NaNO_3$ increases with the soluble salt content of the BW. $NaNO_3$ leach rates for STE3 0.5 N samples are, respectively, equal to 0.08, 0.02 and 0.02 in solutions of chemical activities equal to 1, 0.95 and 0.9. In comparison, $NaNO_3$ leach rates for STE3 1 N samples in the same conditions are equal to 0.14, 0.06 and 0.06. These tendencies are consistent with Eq. (29) in Part I which specifies similar impacts of the chemical activity gradient and of the soluble salt content on the $NaNO_3$ release rates.

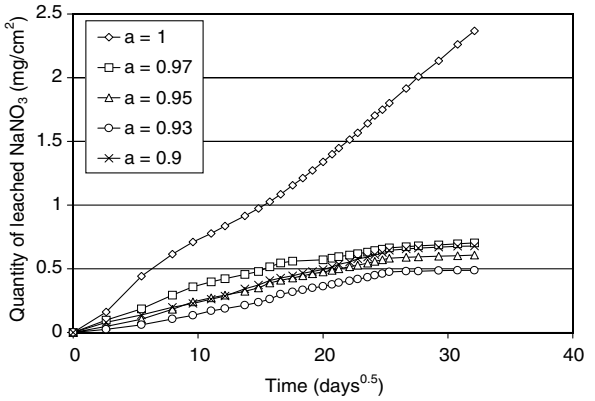

Fig. 8. Release of $NaNO_3$ from STE3 0.5 N samples leached by solutions in which the chemical activity of water a_o varies between 0.9 and 1.

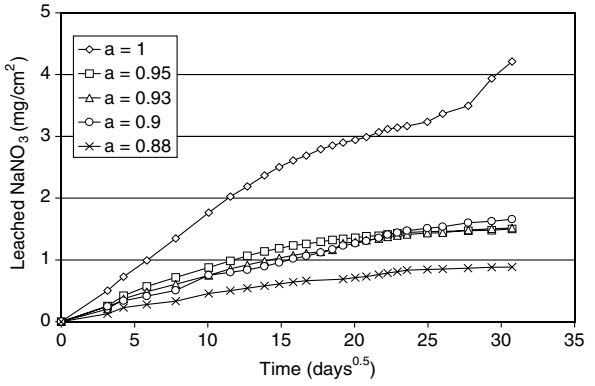

Fig. 9. Release of $NaNO_3$ from STE3 1 N samples leached by solutions in which the chemical activity of water a_o varies between 0.88 and 1.

4. Pore structure of the permeable layer

4.1. Duration of leaching

The first parameter which has been studied is the duration of leaching. To this end, ESEM observations have been performed on STE3 0.5 N samples leached by pure water during 2, 6, 12, 25 and 37 months. The resulting binary images are displayed in Fig. 10. They illustrate the progression in time of the permeable layer in the BW samples. The pores appear to be uniformly distributed with a tendency for bigger pores to concentrate near the leached surface. The maximum diameter of the pores reaches 100–200 μm. Mean porosity profiles (average of three porosity profiles) for each date are represented in Fig. 11.

Qualitatively, the porosity profiles obtained after different leaching durations have a similar aspect. The maximum porosity (fairly constant in time and equal to 55–60%) is obtained at or near the leached surface (depth = 0). It is followed by a continuous and pronounced decrease of the porosity when progressing in the depth of the permeable layer. Finally at some stage, the measured pore volume reaches zero.

4.2. Chemical activity of water in the leachant and soluble salt content

The second parameter which has been studied is the chemical activity of water in the leachant. To this end, ESEM observations have been performed on STE3 0.5 N and STE3 1 N BW samples in contact during 11 months with leachants of chemical activities equal to 0.74, 0.89, 0.96 and 1. The porosity profiles (average of three porosity profiles) for

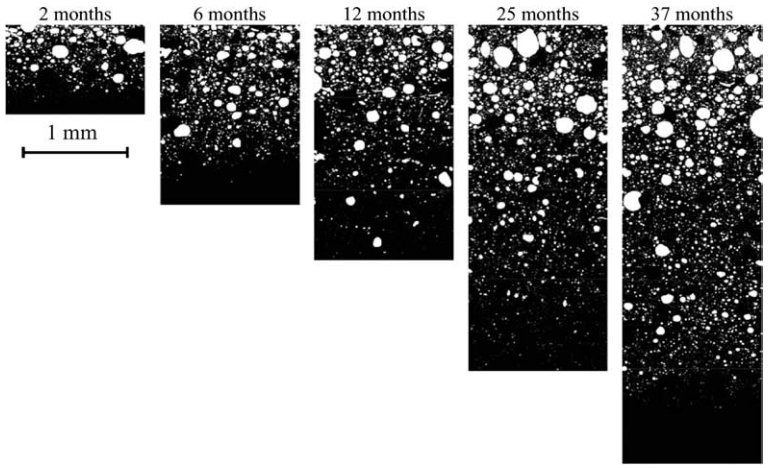

Fig. 10. Binary images based on ESEM observations performed on STE3 0.5 N samples leached by pure water during 2, 6, 12, 25 and 37 months.

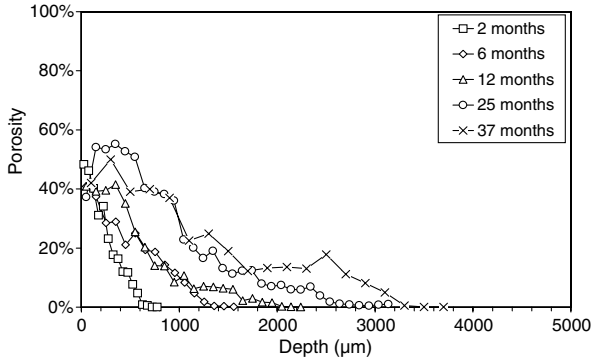

Fig. 11. Porosity profiles obtained from ESEM observations of STE3 0.5 N samples leached by pure water during 2, 6, 12, 25 and 37 months.

each leaching conditions are displayed in Figs. 12 and 13, respectively, for the STE3 0.5 N and STE3 1 N samples.

Obviously, the porosity profiles of Figs. 12 and 13 are comparable to those presented previously in Fig. 11. They exhibit a maximum at or near the leaching surface and decrease continuously when progressing in the depth of the permeable layer. However, the STE3 1 N porosity profiles of Fig. 13 differ from those of Figs. 11 and 12 obtained on STE3 0.5 N samples since they end up with a pronounced slope, which may be considered as a front. This difference might be due to the more important porosity that results theoretically from the dissolution of a more important quantity of soluble salts per unit volume of BW, see Eq. (13)

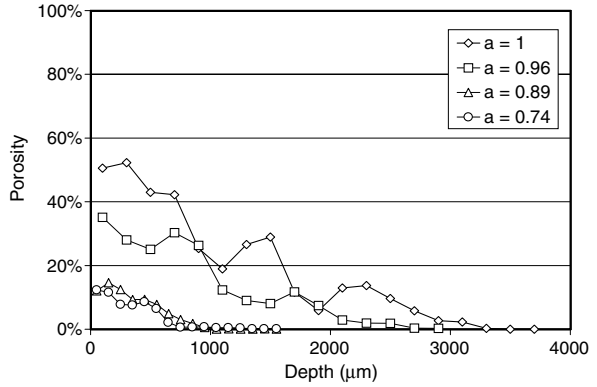

Fig. 12. Porosity profiles obtained from ESEM observations performed on STE3 0.5 N samples leached 11 months by solutions of chemical activities equal to 0.74, 0.89, 0.95 and 1.

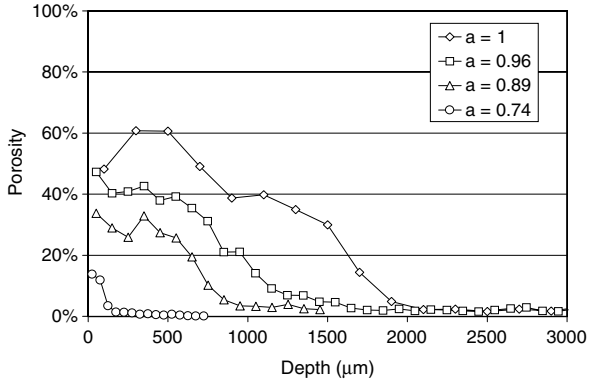

Fig. 13. Porosity profiles obtained from ESEM observations performed on STE3 1 N samples leached 11 months by solutions of chemical activities equal to 0.74, 0.89, 0.95 and 1.

in Part I. A greater discontinuity in porosity may therefore appear more clearly in ESEM image analysis.

5. Simulations with the analytical and COLONBO models

In this section, numerical simulations are performed with the COLONBO model (see Part I for a description of the model). Since the diffusion coefficients of water and salts utilized in the COLONBO model are unknown, the experimental water uptake and $NaNO_3$ release rates presented in Part III (see Figs. 6 and 7 for water uptake and Figs. 8 and 9 for sodium nitrate release) are used to estimate these parameters. Inverse analysis assuming square root of time kinetics laws leads to the diffusion coefficients of Table 4.

Apart from the diffusion coefficients of water and salts in the permeable layer, the other material parameters employed in the COLONBO simulations are constant and take the following values: water diffusion coefficient in bitumen, $D_{w,b}^{eff} = 1.10^{-15}$ m^2/s, solubility of water in bitumen $\phi_b = 5\%$, total salt contents, 38% for STE3 0.5 N and 42% for STE3 1 N, mass density 1400 kg/m^3, soluble salt content $f_s = 8.6\%$ for STE3 0.5 N and $f_s = 17\%$ for STE3 1 N, activity coefficient for water $\gamma_w = M_w/\rho_w$ with $M_w = 0.018$ kg/mol and $\rho_w = 1000$ kg/m^3. Note that the diffusion coefficients of Table 4 are consistent with experiment measures obtained on leached BW samples using diffusion cells and radioactive tracers [15].

Finally, to demonstrate the validity of the analytical expressions derived in Part I of this paper, porosity profiles are also calculated thanks to these expressions. To this end, Eq. (25) (see Part I) is first used to estimate the thickness of the permeable layer X_d. The chemical activity profile in the permeable layer is then obtained according to Eq. (22) (see Part I). The porosity profile is finally estimated thanks to Eq. (13) (see Part I).

Table 4
Diffusion coefficients used in the COLONBO simulations, based on the fitting of the experimental water uptake and $NaNO_3$ leach rates

Leachant activity	0.9	0.95	1
STE3 0.5 N			
Diffusivity of water (10^{-13} m^2/s)	0.3	0.3	0.7
Diffusivity of salts (10^{-15} m^2/s)	0.2	0.2	0.6
STE3 1 N			
Diffusivity of water (10^{-13} m^2/s)	0.4	0.4	0.9
Diffusivity of salts (10^{-15} m^2/s)	0.5	0.4	1.2

5.1. Duration of leaching

The porosity profiles obtained after 2, 6, 12, 25 and 37 months leaching according to the COLONBO model and the analytical solution presented in Part I of this paper, are shown in Fig. 14. The profiles are calculated using the water and salt diffusion coefficients given in Table 4 for the STE3 0.5 N BW samples and for a leachant activity equal to 1.

The porosity profiles obtained with the COLONBO model ('COLONBO') and the analytical expressions ('analytical') show many similarities with the experimental ones (see Fig. 11). They are characterized by a maximum porosity near the leached surface (58% for the COLONBO profiles, 78% for the analytical profiles), independent of time, and a progressive decrease of the pore volume in the depth of the permeable layer. The analytical porosity profiles tend however to overestimate the maximum porosity at the leached surface (55–60% in the experiments). This overestimation is due to the assumption of a constant (in time) soluble salt content in the BW, assumption used to solve analytically the constitutive equations describing the leaching of BW materials. The lack of soluble salt diffusion results in fact in a more important water demand per unit volume of unleached BW during the progression of the permeable layer. In consequence, as illustrated in Fig. 14, for a given water uptake rate, the progression of the permeable layer

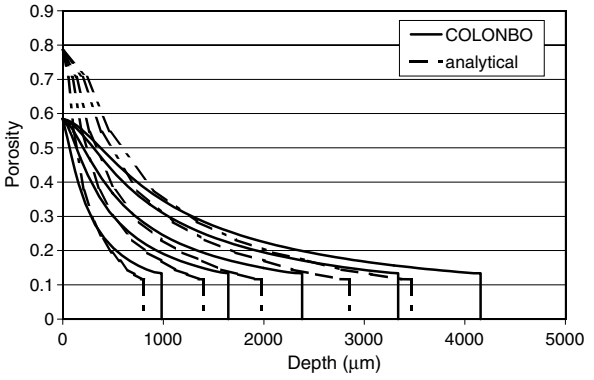

Fig. 14. Porosity profiles for STE3 0.5 N samples leached by pure water during 2, 6, 12, 25 and 37 months, according to the COLONBO model and the analytical expressions 13, 22 and 25 presented in Part I of this paper.

according to the analytical solution is slightly slower than that obtained with the COLONBO model.

To compare more precisely the different porosity profiles, the evolution of the apparent thickness of the permeable layer can be plotted in function of time, as shown in Fig. 15. For the analytical and numerical results of Fig. 14, the apparent thickness of the permeable layer is obtained from the position of the soluble salt dissolution front. Since this front does not appear clearly in the experimental profiles of Fig. 11, the estimation of the thickness of the permeable layer is based on the depth at which pore volume equals zero.

Obviously, the evolution of the experimental apparent thickness of the permeable layer is proportional to the square root of time with a rate close to 100 μm/days$^{0.5}$, see the linear regression on experimental results presented in Fig. 15. This result is consistent qualitatively (square root of time dependency, see Eq. (25) in Part I) and quantitatively with the numerical and analytical estimations, even if the dissolution front does not exist in the experimental profiles of Fig. 11. Note furthermore that the difference between the numerical and the analytical estimations of the apparent thickness of the permeable layer is small. This result demonstrates that the impact of salt diffusion on porosity profiles is mainly localized near the leached surface.

5.2. Chemical activity of water in the leachant and soluble salt content

To estimate precisely the impact of the chemical activity of water in the leachant on the pore structure of leached BW samples, the maximum porosity and the apparent thickness of the permeable layer obtained from the porosity profiles of Figs. 12 and 13 are plotted in Figs. 16 and 17, respectively. These results are compared in the same Figures to those obtained with the numerical model COLONBO and the analytical expressions derived in Part I of this paper. The water and salt diffusion coefficients given in Table 4 for leachant activities equal to 1, 0.96 (0.95 in Table 4) and 0.89 (0.9 in Table 4) were used in the simulations and the analytical calculations. No simulations were however performed for

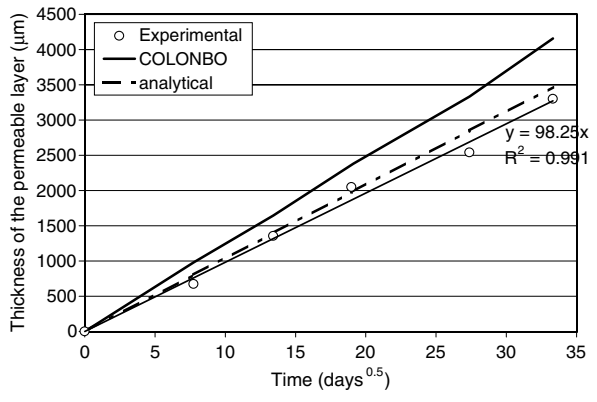

Fig. 15. Evolution of the thickness of the permeable layer with the duration of leaching for STE3 0.5 N samples leached by pure water, as obtained from the experimental, numerical (COLONBO) and analytical porosity profiles.

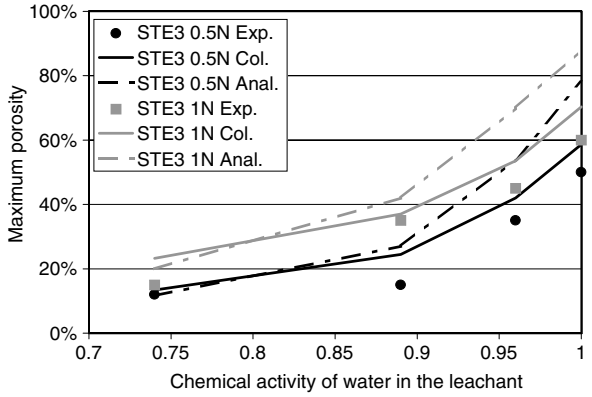

Fig. 16. Evolution of the maximum porosity with the chemical activity of water in the leachant for STE3 0.5 N and STE3 1 N samples leached during 11 months, as obtained from the experimental, numerical (COLONBO) and analytical porosity profiles.

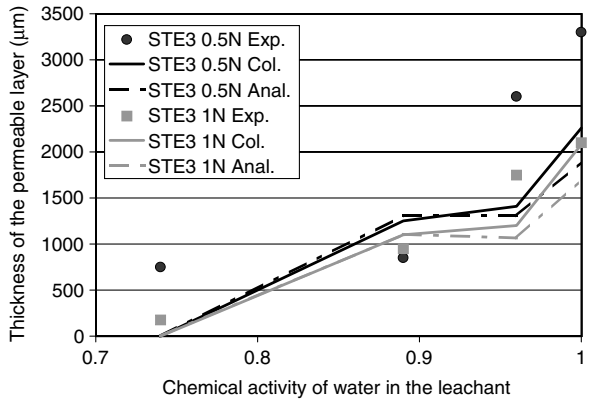

Fig. 17. Evolution of the thickness of the permeable layer with the chemical activity of water in the leachant for STE3 0.5 N and STE3 1 N samples leached during 11 months, as obtained from the experimental, numerical (COLONBO) and analytical porosity profiles.

the leachant activity equal to 0.74 since, in theory, the chemical activity gradient in the permeable layer, which governs its progression, equals zero in this case.

All the results presented in Fig. 16 show that the maximum porosity increases with the chemical activity of water in the leachant. The rise of the experimental, COLONBO-based, and analytical maximum porosities appears particularly important when the chemical activity of water in the leachant exceeds 0.95. This evolution can be attributed to the more important quantity of water that is needed to achieve a given equilibrium in the solution-filled pores of the permeable layer when the leachant's activity increases. The comparison between the experimental profiles for the STE3 0.5 N (black circles in Fig. 16) and STE3 1 N (grey squares in Fig. 16) samples indicates that, independent of the leachant's activity, the maximum porosity increases with the soluble salt content. This is completely consistent with the numerical and analytical trends which show that the higher the soluble salt loading, the greater the quantity of water needed to dissolve all the salts contained per unit volume of BW and hence the greater the porosity.

According to the numerical model COLONBO and the analytical trends derived in Part I of this paper, the apparent thickness of the permeable layer at a given time should theoretically increase with the water activity gradient and decrease with the soluble salt content. The correctness of these tendencies is confirmed by the experimental results shown in Fig. 17. For STE3 0.5 N samples (black circles in Fig. 17), the apparent thickness varies between 750 and 3300 μm when the activity of water in the leachant increases from 0.74 to 1. By comparison, for STE3 1 N samples (grey squares in Fig. 17), the apparent thickness changes from 175 to 2100 μm for the same leachants.

6. Conclusions

In this paper, the behaviour of leached bituminized waste materials and the development of a saline solution-filled pore structure has been studied. The impact of material (soluble salt content) and environmental parameters (chemical activity of water in the leachant) on leaching kinetics has been investigated experimentally. Standard leach tests with periodic measures of the water uptake and of the release of $NaNO_3$ have been carried out. To quantify the evolution of the permeable layer which forms in leached BW materials and to estimate the pore volume and pore distribution in this layer, an innovative approach based on ESEM image analysis has been developed and applied to leached BW samples. Experimental results demonstrate that:

- the apparent thickness of the permeable layer which forms in leached BW materials evolves proportionally to the square root of time. Its size decreases with increasing soluble salt contents and increases with the chemical activity of water in the leachant,
- the porosity in the permeable layer is not constant; the maximum porosity is situated near the leached surface and depends on the chemical activity of water in the leachant,
- the water uptake follows a square root of time law, increases both with the soluble salt content of the BW materials and with the chemical activity of water in the leachant,
- the soluble salt release (assimilated to sodium nitrate in the model) evolves also proportionally to the square root of time; it increases with the soluble salt content of the BW materials and with the chemical activity of water in the leachant.

These results and experimental trends are consistent in all points with those obtained from the constitutive model COLONBO and the analytical expressions presented in Part I of this paper. Indeed, reasonably good estimates for all measurable leaching indicators (thickness of the permeable layer, water uptake, soluble salt release, porosity of the permeable layer) and their evolution with material (soluble salt content) and environmental parameters (chemical activity of water in the leachant) have been obtained from the numerical and analytical calculations.

Acknowledgement

The authors would like to acknowledge AREVA-COGEMA for their financial support to this research.

References

[1] H. Sorantin, I. Huber, H. Jakusch, K. Knotik, Nucl. Eng. Des. 34 (1975) 439.
[2] F. Lanza, H. Manaktala, T. Visani, Eur. Appl. Res. Rept. Nucl. Sci. Technol. 5 (3) (1983) 325.

[3] J. Timulak, J. Radioanal. Nucl. Chem. 129 (2) (1989) 273.
[4] K. Brodersen, G. Brunel, R. Gens, F. Lambert, J.C. Nominé, A. Sneyers, P. Van Iseghem, Final Report for Contract No. F12W-CT-91-0025, EUR 18228 EN, Luxembourg, 1998.
[5] J.-W. Lee, Y.-G. Ryue, K.-H. Kim, Proceedings of the International Conference on Waste Management, Tucson, March 1–5, American Nuclear Society, 1998.
[6] A. Sneyers, P. Van Iseghem, Mater. Res. Soc. Symp. Proc. 506 (1998) 565.
[7] K. Brodersen, in: R. Vanbrabant, P. Selucky (Eds.), Proceedings of the International Workshop on the Safety and Performance Evaluation of Bituminization Processes for Radioactive Waste, Nuclear Research Institute Rez, Czech Republic, 1999, p. 149.
[8] I.A. Sobolev, A.S. Barinov, M.I. Ojovan, N.V. Ojovan, I.V. Startceva, Z.I. Golubeva, in: R. Vanbrabant, P. Selucky (Eds.), Proceedings of the International Workshop on the Safety and Performance Evaluation of Bituminization Processes for Radioactive Waste, Nuclear Research Institute Rez, Czech Republic, 1999, p. 131.
[9] E. Valcke, A. Sneyers, P. Van Iseghem, in: R. Vanbrabant, P. Selucky (Eds.), Proceedings of the International Workshop on the Safety and Performance Evaluation of Bituminization Processes for Radioactive Waste, Nuclear Research Institute Rez, Czech Republic, 1999, p. 137.
[10] T. Yamaguchi, T. Amaya, A. Mukunoki, M. Fujiso, in: R. Vanbrabant, P. Selucky (Eds.), Proceedings of the International Workshop on the Safety and Performance Evaluation of Bituminization Processes for Radioactive Waste, Nuclear Research Institute Rez, Czech Republic, 1999, p. 161.
[11] I.A. Sobolev, A.S. Barinov, M.I. Ojovan, N.V. Ojovan, I.V. Startceva, Z.I. Golubeva, Mater. Res. Soc. Symp. Proc. 608 (2000) 571.
[12] M. Pettersson, M. Elert, Characterisation of bitumenised waste in SFR 1, SKB Report R-01-26, June 2001.
[13] S. Nakayama, Y. Iida, T. Nagano, T. Akimoto, J. Nucl. Sci. Technol. 40 (4) (2003) 227.
[14] B. Gwinner, B. Simondi-Teisseire, I. Félines, P. Frugier, E. Ringot, Visualisation Image Modélisation, Récents Progrès en Génie des Procédés 78 (15) (2001) 369.
[15] B. Gwinner, Comportement sous eau des déchets radioactifs bitumés: validation expérimentale du modèle de dégradation COLONBO, PhD thesis (in French), Institut National Polytechnique de Lorraine, Nancy, France, 2004.
[16] S. Beucher, Scan. Microsc. Int. (Suppl. 6) (1992) 299.